ELSEVIER

Chemical Engineering Journal 108 (2005) 227–237

Chemical Engineering Journal

www.elsevier.com/locate/cej

# Cycling effects on the methane regeneration kinetics of CuO/γ-$Al_2O_3$ sorbent

Krzysztof Piotrowski [a,b], Tomasz Wiltowski [a,c,*], Tomasz Szymański [c], Kanchan Mondal [c], Vishnuraj Rathinaswamy [c], Ronald W. Breault [d], Lubor Stonawski [a,c]

[a] *Coal Research Center, Southern Illinois University Carbondale, Carbondale, IL 62901, USA*
[b] *Department of Chemical and Process Engineering, Silesian University of Technology, Gliwice, Poland*
[c] *Department of Mechanical Engineering and Energy Processes, Southern Illinois University Carbondale, Carbondale, IL 62901, USA*
[d] *US Department of Energy, Morgantown, WV, USA*

Received 29 September 2004; received in revised form 9 February 2005; accepted 15 February 2005

**Abstract**

Due to the excellent adsorption capacity coupled with convenient regeneration characteristics demonstrated by copper oxide impregnated γ-$Al_2O_3$ spheres this process has the potential of being more effective, feasible and widely accepted over the lime and limestone scrubbing in the removal of $SO_2$. Thermogravimetric tests concerning the copper oxide on γ-$Al_2O_3$ (both fresh and spent) sorbent regeneration kinetics by methane were performed. Commercially available (SELEXSORB$^{TM}$) 1/8 in. diameter γ-$Al_2O_3$ spheres loaded with 5.8 wt.% of Cu were used for these studies. The regeneration experiment temperatures were: 700, 727 and 750 K, while a 20 $cm^3$/min flow of pure methane was applied. To determine the reaction mechanism and its kinetic parameters evaluation, the TGA data were subjected to a rigorous series of theoretically developed models of topochemical reaction kinetics. Hancock and Sharp's tabulations were used to establish the reaction mechanisms and their rate constants evaluation. The various diffusion kinetic equations found themselves useful for the description of the reaction time—courses in the final stage of each experiment.


*Keywords:* Copper oxide; Methane; Regeneration; Topochemical reaction kinetics

## 1. Introduction

Sulfur dioxide ($SO_2$) and nitrogen oxides ($NO_x$) are common air pollutants which have to be removed before emitting the flue gases to the atmosphere. The copper oxide on γ-$Al_2O_3$ support has received a great attention as a low-temperature catalyst since it is capable of removing $SO_2$ and $NO_x$ from flue gases simultaneously as well as having the ability to regenerate relatively easily under reducing conditions (releasing chemisorbed $SO_2$) [1–6]. Its stability is relatively high during the process followed by regeneration in the cyclic operation mode. The copper oxide (CuO) is converted to copper sulfate ($CuSO_4$) by the following reactions with $SO_2$ and $O_2$ (de$SO_2$ mode, Eqs. (1) and (2):

$$SO_2 + \tfrac{1}{2}O_2 \xrightarrow{CuO} SO_3 \quad (1)$$

$$SO_3 + CuO \rightarrow CuSO_4 \quad (2)$$

The reduction of nitric oxides (NO, $NO_2$) to harmless $N_2$, using $NH_3$ as the reducing agent, is then selectively catalyzed by the surface layer of $CuSO_4$ (mainly) as well as the unreacted CuO (de$NO_x$ mode, Eqs. (3) and (4):

$$4NO + 4NH_3 + O_2 \xrightarrow{CuO-CuSO_4} 4N_2 + 6H_2O \quad (3)$$

$$2NO_2 + 4NH_3 + O_2 \xrightarrow{CuO-CuSO_4} 3N_2 + 6H_2O \quad (4)$$

The sulfated copper oxide on γ-$Al_2O_3$ sorbent can be regenerated either by the thermal decomposition (this method causes decrease of the de$SO_2$ activity) or with some reducing agent (e.g. $H_2$, CO or $CH_4$) with the evolution of a concen-

* Corresponding author. Tel.: +1 618 453 7346; fax: +1 618 453 7346.
*E-mail address:* tomek@siu.edu (T. Wiltowski).

1385-8947/$ – see front matter © 2005 Elsevier B.V. All rights reserved.
doi:10.1016/j.cej.2005.02.026

**Nomenclature**

| | |
|---|---|
| $\Delta E_a$ | activation energy (kJ/mol) |
| $k$ | kinetic constant ($s^{-1}$) |
| $m$ | sample mass (g) |
| $m$ | constant associated with the geometry of the system |
| MD | mean deviation |
| $n$ | number of experimental data considered |
| $R$ | regression correlation coefficient |
| RMSD | root mean square deviation |
| $t$ | process time (s) |
| $T$ | process temperature (K) |

*Greek letters*

| | |
|---|---|
| $\alpha$ | fraction reacted in time $t$ (thus, conversion degree for the time $t$) |
| $\beta$ | constant, partially depended both on nucleation frequency and the rate of grain growth |

*Superscripts*

| | |
|---|---|
| calc | value calculated by selected model |
| exp | experimental value |
| 0 | initial |

trated stream of $SO_2$ (>30%), convertable to sulfuric acid or elementary sulfur (reductive regeneration mode, Eqs. (5)–(7) [7–9]:

$$CuSO_4 + 2H_2 \rightarrow Cu^0 + SO_2 + 2H_2O \quad (5)$$

$$CuSO_4 + 2CO \rightarrow Cu^0 + SO_2 + 2CO_2 \quad (6)$$

$$CuSO_4 + \tfrac{1}{2}CH_4 \rightarrow Cu^0 + SO_2 + \tfrac{1}{2}CO_2 + H_2O \quad (7)$$

The partially regenerated sorbent ($Cu^0$ supported on γ-$Al_2O_3$) is then oxidized to CuO before commencing a new reaction-regeneration cycle (oxidation mode, Eq. (8)):

$$Cu^0 + \tfrac{1}{2}O_2 \rightarrow CuO \quad (8)$$

Copper oxide dispersed on alumina support has a large specific surface area (in fresh sorbent it ranges from 117 $m^2/g$ up to 230 $m^2/g$ of sorbent; however, the 132–153 $m^2/g$ range is always prevalent) with sufficiently large pore volume and an uniform pore distribution [10]. The large specific surface area of the support is an essential factor for enhancing the loading of Cu species, thus resulting in enhanced $SO_2$ sorption capacity [11]. This way the dispersed CuO possesses a rigid, mechanically strong support, which is thermally and chemically resistant to the harsh conditions encountered in the flue gas desulfurization processes. Moreover, a fast sulfation and regeneration kinetics is observed. Macken et al. [1,9] indicated that several chemical transformations occur during the cyclic operation of sulfation–regeneration–oxidation ($CuO \rightarrow CuSO_4 \rightarrow Cu^0 \rightarrow CuO$), and thus, the CuO on γ-$Al_2O_3$ catalyst requires exceptional physicochemical and mechanical properties that should remain stable over a large number of sulfation–regeneration cycles.

Since the introduction of the Shell flue gas desulfurization process (removal of $SO_2$ from flue gases with a copper oxide catalyst employing two reactors in the $SO_2$ capture-catalyst regeneration swing operation regime) in the late 1960s, a significant amount of research has been conducted to improve the process, including its regeneration [7–9]. Although the regeneration with $CH_4$, as opposed to $H_2$, is relatively slow and is strongly inhibited by the $SO_2$ released (counterdiffusion effects) and requires higher temperature range (by ca. $\Delta T = 150$ K (lower reducing activity), fewer unwanted side-reactions occur (especially the formation of CuS and $Cu_2S$, producing $H_2S$ and lowering the amount of $SO_2$ sorbed by the CuO on γ-$Al_2O_3$ catalyst in the following cycles) that would require additional pollution control units [9]. When $CH_4$ is employed as the reducing agent, $SO_2$ is the only sulfur containing species detected in the gas stream [12]. Moreover, working at high temperatures (Sulfation–Regeneration Integration Technology) with $H_2$ is dangerous. McCrea et al. [13] reported that temperatures in excess of $T = 673$ K are required for the efficient regeneration of the sulfated CuO on γ-$Al_2O_3$ catalyst with $CH_4$ (close to the temperature range of the sulfation process). They also reported that the regeneration rate was strongly dependent on temperature. Reducing power of different species ($H_2$, $CH_4$, $C_3H_8$ and $NH_3$) is also reported by Macken et al. [9].

The task undertaken in this work is a kinetic study of the first stage of regeneration of CuO on γ-$Al_2O_3$ sorbent with methane ($CuSO_4 \rightarrow Cu^0$, see Eq. (7)). This key-process step influences the overall de$SO_2$–de$NO_x$ process economics and feasibility. This sorbent has a great potential to become a key-factor in the successful commercially proecological technology as an improved alternative to the conventional limestone scrubbing, which currently dominates the post combustion flue gas cleanup of sulfur dioxide.

There is little data published concerning the regeneration kinetics. Early fixed-bed tests performed by McCrea et al. [13] demonstrated a slow regeneration with $CH_4$ at $T = 673$ K. It was reported, that the nearly complete sulfur removal was obtained after $t = 30$ min at $T = 723$ K and in less than $t = 10$ min at $T = 773$ K. The sorbent retained about 1% S even after prolonged ($t = 60$ min) exposure to $CH_4$ at $T = 773$ K. The sulfur, however, was probably strongly bound to the γ-$Al_2O_3$ support and did not affect the capacity of the CuO for subsequent $SO_2$ removal. Studies by Yeh et al. [14] in a microbalance reactor showed an 80% reduction of $CuSO_4$ with $CH_4$ in $t = 10$ min at $T = 723$ K or in $t = 25$ min at $T = 673$ K. The rates of reaction evaluated during this study were several times larger than those reported by McCrea et al. [13], probably due to a much larger excess of $CH_4$ used in the microbalance tests. McCrea et al. [15] found the rate of regeneration reaction to be strongly dependent on temperature while relatively independent of methane concentration. In the tests employing a large (1.2 $m^3$) fluidized-bed adsor-

ber that was operated with a continuous solid solids feed at a constant flowrate, the spent sorbent was collected and regenerated batchwise in a static bed at $T = 693$ K (Yeh et al. [16]). Methane flow was continued until there was no more reaction progress (the regenerated sorbent had about 1 wt.% S).

Centi et al. [17] observed that the $deSO_2$ activity of CuO on $\gamma$-$Al_2O_3$ sorbent is maintained up to 10 cycles of sulfation and regeneration (temperature of sulfation = 573 K, temperature of regeneration = 743 K). Yoo et al. [8] reported that the sulfur removal capacity of the surface-sulfated sorbent (temperature of sulfation = 573 K, temperature of regeneration = 773 K) decreased after ca. 2 cycles and remained constant until the cycle number reached the value of 7. These authors performed the cyclic sulfation–regeneration tests (temperature of sulfation = 773 K, equals to the temperature of regeneration = 773 K) up to 30 times. It was reported that the sulfur removal capacity of the sorbent decreased only slightly after 30 cycles. They concluded that the degradation of the active sites of the sorbent occurs beyond the $T = 773$ K. The completion of the regeneration reaction could not be achieved even at $T = 773$ K due to the presence of the residual surface sulfur compounds on the alumina support ($Al_2(SO_4)_3$, $Al_2S_3$) [8]. Additional trials showed that the sulfur removal capacity does not decrease until the number of sulfation–regeneration (both processes at $T = 713$ K) cycles reaches a value of 30. It clearly demonstrated that the reaction temperature plays an important role in the deactivation of active sites on the sorbent structure. This degradation of active sites can be avoided applying the lower temperature of the process. Harriott and Markussen [7] reported the kinetic test results with $CH_4$–$SO_2$–$N_2$ mixtures (of 5–100% $CH_4$) within the $T = 723$–$783$ K window. The supported CuO was exposed to two cycles of $SO_2$ sorption coupled with the $CH_4$ regeneration, followed by a final sulfation step. The sulfation steps were conducted at $T = 673$ K. Wang and Lin [3] applied 15 consecutive cycles of sulfation–reduction–oxidation (28 days).

A relatively small number of studies were oriented to the stability of the CuO on $\gamma$-$Al_2O_3$ catalyst over the extended sulfation–regeneration cyclic treatment. Macken et al. [1] tested a series of CuO on $\gamma$-$Al_2O_3$ catalysts which were subjected to a large number (36–1525) of the consecutive sulfation–regeneration cycles (temperature of sulfation = 623 K, temperature of regeneration = 773 K) in a quartz fixed-bed reactor. The $SO_2$ sorption capacity of one sample which had been subjected to 1525 cycles was reduced by about 25%, but generally there was no significant change in the reactivity. Johannes et al. [18] tested the catalyst over 800 consecutive sulfation–regeneration cycles in a fixed-bed reactor. McCrea et al. [13] tested the sorbent for over 200 sulfation–regeneration cycles in a fixed-bed bench-scale reactor. After the tests, there was no evidence of chemical or physical deactivation. Yeh et al. [16] tested the same catalyst for 75 sulfation–regeneration cycles in a fluidized bed reactor. They concluded that, there was no evidence of any decrease in the chemical activity of the sorbent after the 75 cycles. Kiel et al. [19] tested the regeneration kinetics of several silica-supported copper oxide sorbents in a microbalance device within the temperature window $T = 573$–$723$ K. Even after 75 cycles of oxidation, sulfation and reduction the sorbents did not show a significant loss in the chemical activity except for some evidence of deactivation within the first 1–3 cycles. The $deSO_2$ process kinetics on the sorbent was found to be in agreement with the literature data reported for the alumina-supported CuO sorbents.

For the sulfated ion-exchanged sorbents, the reduction by hydrogen was identified as an autocatalytic reaction. The autocatalytic effect was also observed during the (much slower) reduction by methane, but there it was preceded by a period in which a second autocatalytic effect appeared. Jeong and Kim [20] investigated the cyclic effects on the regeneration quality and efficiency (temperature of sulfation = 573–773 K, temperature of regeneration = 693–773 K) with LiCl and NaCl introduced as structural additions. They provided the strong analytical and experimental proof that the main changes in the sorbent's capacity take into effect within the first 10 cycles, when the surface morphology stabilizes and provides the steady-state conditions for these heterogeneous processes during the next cyclic operations. In the tests with 50 and 100 vol.% of $CH_4$ Yeh et al. [14,21] observed the regeneration rate to be first-order with respect to $CH_4$.

Harriott and Markussen [7] proposed and applied the first-order kinetics coupled with a Langmuir–Hinshelwood model. The kinetic tests showed, that the rate of regeneration with $CH_4$ is strongly inhibited by the product gases, particularly $SO_2$. Chen and Yeh [22], using natural gas as an effective reducing agent, enhanced this description introducing the possibility of deviation from the first-order kinetics with respect to copper sulphate and applying the influence of the mass transfer limitations. The tests performed evaluated the effects of: process temperature, methane to copper sulfate feed ratio and the sorbent's residence time. The regenerator modeling also details the impact of the mass transfer resistances (gas velocity effects) on the reactor's performance. Macken et al. [9] and Yoo et al. [8] presented only a qualitatively description of the results without the kinetic analysis.

It can be concluded, that in the accessible literature there is no reported any work concerning the application of the topochemical models for the description and interpretation of the regeneration kinetics data. Since in this reaction system, there are complex phase transformations ($CuO \rightarrow CuSO_4 \rightarrow Cu^0 \rightarrow CuO$) the authors have applied the topochemical approach to interpret the kinetics for these reaction ($CuSO_4 \rightarrow Cu^0$, see Eq. (7)). Based on past studies reported in literature, the experiments were conducted at temperatures ranging from 700 to 750 K (since $T = 773$ K corresponds to loss of the catalytic activity of the sorbent, while $T = 673$ K corresponds to a low reduction rate) while 10 cycles was regarded as sufficient (since the main morphology transformations are reported within the first 10 cycles after which there is an evident stabilization in the catalyst performance [8]).

## 2. Experiments

The commercial copper impregnated γ-alumina spheres SELEXSORB$^{TM}$ (1/8 in. diameter) were obtained from Aluminum Company of America (ALCOA). The copper loading in the fresh sorbent was 5.8 wt.% (as determined by a Perkin-Elmer Inductively Coupled Argon Plasma 400 Emission Spectrometer). Certified gas cylinders of $SO_2$, $CH_4$ and air were obtained from Airgas, Inc. (Radnor, PA). The flowrates of these gases were maintained using mass flow controllers. The specific surface area of both the fresh sorbent and the sorbent at different intervals in the sulfation/regeneration cycle were determined with the use of Quantachrome Instruments NOVA–1200 BET Surface Area Analyzer (the three point BET procedure applied, nitrogen adsorption at $T = 77.4$ K).

Since the main objective of the work [23] was to analyze the sorbent's regeneration capabilities after several cycles of sulfation and regeneration—the kinetic study evaluated the sorbents in three stages of their life, namely: the fresh sorbent, sorbent after five cycles (intermediate) of sulfation/regeneration and heavily cycled sorbent.

The initial activation of the sorbent was performed in a Thermolyne F 21100 Tube Furnace (single set point temperature control) in a pure methane atmosphere at $T = 750$ K. The sample was placed in the required temperature zone inside the tube furnace. Following the activation, the sorbent was sulfated in a tube furnace (the process temperature $T = 750$ K). The $SO_2$ concentration in the $SO_2$/air mixture used was 20,000 ppm. A pulsed fluorescent analyzer (capable of measuring of the $SO_2$ concentration within the 0.2–5000 ppm range) connected to the tube furnace exhaust through the Heated Sample Gas Dilution and Conditioning Unit (diluted by nitrogen) Model 900 provided by Thermo Electron Corporation was used. Sulfation of the sorbent's sample continued till its entire capacity was exhausted (as indicated when the $SO_2$ concentrations in the inlet and outlet are equal).

The heavily cycled sorbent was obtained directly from the pilot plant located in Southern Illinois University Carbondale—Coal Research Center Industrial Park, Carterville, IL, USA. This sorbent had gone through the repetitive cycles of sulfation and regeneration for ca. $t = 800$ h of operation (10 cycles).

The kinetic data presented in this work, concerning the methane regeneration step (Eq. (7)), were obtained using a Perkin-Elmer TGA-7 thermogravimetric analyzer (analytical precision of $10^{-6}$ g) equipped with the standard stainless steel pan and connected with the computer data acquisition system. The TGA technique was consciously used by the authors instead of the microreactor device since the eventually occurred inherent gradients of gas and sample's composition along the reactor's working volume could cause the interpretation of the results more complex and ambiguous (e.g. making allowance for the gas hydrodynamics and flow dispersion, thus deviation from the theoretically convenient plug-flow reactor approximation). The TGA data, involving by nature the uniform gas and solid compositions, as well as their contact interface surface, can be regarded as the more suitable and reliable for these precise kinetic investigations. From the theoretical point of view (thermodynamic and kinetic limitations in the specific process conditions), the decrease in the sample mass resulted only from the $CuSO_4 \rightarrow Cu^0$ chemical transformation, thus could be directly interpreted as the reliable indicator of the reaction (Eq. (7)) course. The regeneration experiments were conducted isothermally at the selected temperatures ranged from 700 to 750 K under pure methane atmosphere ($CH_4$ flow: 20 cm$^3$/min). The methane, as the regeneration gas, was isothermally passed through the uniform sample's powder (sample's initial mass was ca. 12 mg) for about $t = 8$ h till a constant weight was attained (expected sample composition: $Cu^0/\gamma$-$Al_2O_3$). Next, the methane flow was stopped and air was passed for the next 8 h (these data sets are not reported in this work) after which time the sample reached a new constant mass (expected sample composition: $CuO/\gamma$-$Al_2O_3$). The TGA tests were performed in triplicates and the variation in the conversion degree values evaluated (Eq. (9)) ranged within the 2–5% range. No weight fluctuation was reported within the collected data, what speaks well about the stable hydrodynamic flow regime in the analytical TGA device. The initial tests using a little higher flow rates (35 and 40 cm$^3$/min) of the methane confirmed that the effects of external mass- and heat-transfer resistances could be regarded as negligible.

## 3. Discussion of the results

The raw numerical data obtained directly from TGA experiments (microbalance weight loss curves) were recalculated using the Excel$^{TM}$ spreadsheet for the evaluation of conversion degree ($\alpha$) as a function of the process time:

$$\alpha(t) = \frac{m_0 - m(t)}{m_0 - m_{END}} \tag{9}$$

The sulfated sorbent of the initial mass, $m_0$, was exposed to a pure $CH_4$ stream till no further change in weight was detected. It indicated that the regeneration reached the completion and the sample's current mass $m(t)$ reached its final mass $m_{END}$ value (similar to the experimental procedure reported by Harriott and Markussen [7]).

These conversion degree–time data sets were then elaborated according to the Avrami–Erofe'ev method, presented and enhanced by Hancock and Sharp [24–26]. It is a generalized method of comparing the kinetics of the isothermal solid-state reactions, based on the general equation describing nucleation and growth processes, Eqs. (10) and (11):

$$\alpha = 1 - \exp(-\beta t^m) \tag{10}$$

$$\ln(-\ln(1-\alpha)) = \ln\beta + m\ln t \tag{11}$$

where $\alpha$ is fraction reacted till certain process time $t$ (thus, conversion degree for the process time $t$); $\beta$, constant, par-

Table 1
Topochemical reactions kinetic models [24–26]

| Function | Equation | $m$ | Comments |
|---|---|---|---|
| $D_1(\alpha)$ | $\alpha^2 = kt$ | 0.62 | One-dimensional diffusion model (parabolic law) |
| $D_2(\alpha)$ | $(1-\alpha)\ln(1-\alpha)+\alpha = kt$ | 0.57 | Two-dimensional diffusion model (bidimensional particle shape) |
| $D_3(\alpha)$ | $(1-(1-\alpha)^{1/3})^2 = kt$ | 0.54 | Three-dimensional diffusion (Jander's diffusion model, three-dimensional particle shape) |
| $D_4(\alpha)$ | $1-2\alpha/3-(1-\alpha)^{2/3} = k$ | 0.57 | Ginstling and Brounshtein's diffusion model |
| $F_1(\alpha)$ | $-\ln(1-\alpha) = kt$ | 1.00 | First-order reaction model |
| $R_2(\alpha)$ | $1-(1-\alpha)^{1/2} = kt$ | 1.11 | Phase-boundary controlled reaction model (disk), contracting area, i.e. bidimensional shape |
| $R_3(\alpha)$ | $1-(1-\alpha)^{1/3} = kt$ | 1.07 | Phase-boundary controlled reaction model (sphere), contracting volume, i.e. three-dimensional shape |
| $F_0(\alpha)$ | $\alpha = kt$ | 1.24 | Zero-order reaction model |
| $A_2(\alpha)$ | $(-\ln(1-\alpha))^{1/2} = kt$ | 2.00 | Avrami–Erofe'ev model (two-dimensional random nucleation and growth of nuclei) |
| $A_3(\alpha)$ | $(-\ln(1-\alpha))^{1/3} = kt$ | 3.00 | Avrami–Erofe'ev model (one-dimensional random nucleation and growth of nuclei) |

tially depended both on nucleation frequency and grain growth rate; $m$, constant associated with the system geometry.

The kinetic data, which follow any one of the proposed kinetic equations (Table 1), give rise to approximately linear plots of Eq. (11)—on condition that $\alpha$ is limited to the 0.15–0.50 range. The slopes of such plots—thus, the $m$ parameter's values—through comparison with the theoretically expected values (Table 1) can be considered as diagnostic of the reaction mechanism. To determine the reaction mechanism model, as well as for its kinetic parameters evaluation, the TGA data of the form: $\alpha = f(t)$, Eq. (9), were subjected, according to the procedure advocated by Gardner [25], to a rigorous series of these theoretically developed kinetic models, which includes both zero, first or second-order reactions and reactions, whose rates are determined by complex physical processes, such as boundary control, nucleation, growth or various diffusion controlled reactions. Hancock and Sharp's convenient tabulation [24] was used to identify the reaction mechanism and the estimate the reaction rate constants.

The experimental data with the fresh sorbent, recalculated according to Eq. (11), are presented in Fig. 1 as an example. The regression method (the least squares method) was applied. The calculated values of $m$ parameter are presented in Table 2. The controlling reaction mechanism was identified by the comparison of the average $m$ parameter value evaluated numerically with the theoretical ones (see Table 1).

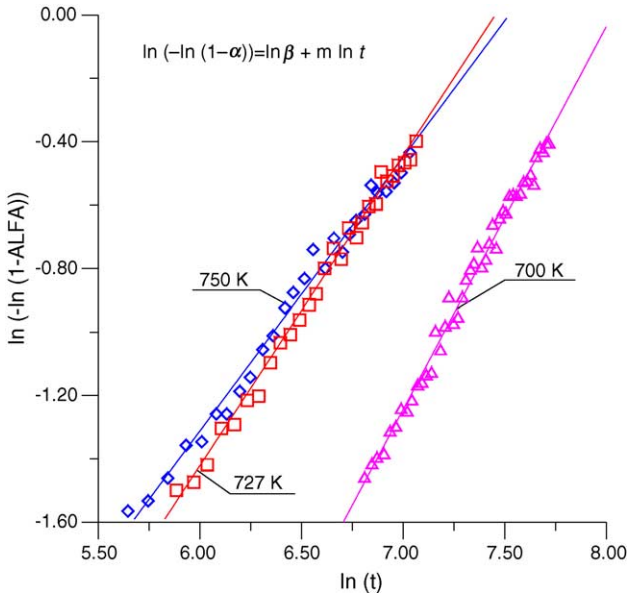


Fig. 1. The $\ln(-\ln(1-\alpha)) = \ln\beta + m\ln t$ equation plots for various process temperatures (700, 727 and 750 K)—$CuO/\gamma\text{-}Al_2O_3$ sorbent (fresh) regeneration by methane.

The fresh sorbent corresponds to the average $m = 1.0156$. The theoretically predicted $m$ parameter's value for a phase-boundary controlled reaction model for a sphere ($R_3$) is 1.07, while that of the first-order kinetics ($F_1$) is 1.00 (see Table 1).

Table 2
Values of $m$ parameter—Hancock and Sharp procedure

| Sorbent type | $T$ (K) | $m$ Eq. (11) | Reg | Number of experimental points |
|---|---|---|---|---|
| Fresh | 700 | 1.2078 | 0.995 | 135 |
| | 727 | 0.9773 | 0.995 | 83 |
| | 750 | 0.8617 | 0.995 | 81 |
| | Average $m = 1.0156$ | | | |
| Intermediate (5 cycles) | 700 | 0.3808 | 0.988 | 112 |
| | 727 | 0.4755 | 0.996 | 61 |
| | 750 | 0.3964 | 0.999 | 100 |
| | Average $m = 0.4176$ | | | |
| Heavy used (10 cycles) | 700 | 2.0090 | 0.997 | 141 |
| | 727 | 1.9964 | 0.997 | 39 |
| | 750 | 2.2065 | 0.995 | 80 |
| | Average $m = 2.0706$ | | | |

Since the statistically estimated $m$ parameter's average value is an intermediate one, the reaction mechanism may be considered to be a combination of the both approaches assumed. The intermediate sorbent provides the $m = 0.4176$. The closest theoretical value are obtained from the diffusion models ($D_1$–$D_4$), covering the range of $m = 0.54$–$0.62$. For the heavy used sorbent, the average value of $m$ was estimated to be 2.07. This value is nearly identical to the Avrami–Erofe'ev model ($A_2$) of the two-dimensional random nucleation and growth of crystals, with the theoretical value of $m = 2.00$.

The slopes of the initial linear portion of the plots of the following kinetic models:

First-order reaction, $F_1(\alpha)$:

$$-\ln(1-\alpha) = kt \tag{12}$$

Phase-boundary controlled reaction model (sphere), $R_3(\alpha)$:

$$1-(1-\alpha)^{1/3} = kt \tag{13}$$

One-dimensional diffusion model (parabolic law), $D_1(\alpha)$:

$$\alpha^2 = kt \tag{14}$$

Two-dimensional diffusion model (two-dimensional particle shape), $D_2(\alpha)$:

$$(1-\alpha)\ln(1-\alpha)+\alpha = kt \tag{15}$$

Three-dimensional diffusion model (Jander's diffusion model, three-dimensional particle shape), $D_3(\alpha)$:

$$(1-(1-\alpha)^{1/3})^2 = kt \tag{16}$$

Ginstling and Brounshtein's diffusion model, $D_4(\alpha)$:

$$\frac{1-2\alpha}{3-(1-\alpha)^{2/3}} = kt \tag{17}$$

Avrami–Erofe'ev model (two-dimensional random nucleation and growth of nuclei), $A_2(\alpha)$:

$$(-\ln(1-\alpha))^{1/2} = kt \tag{18}$$

were numerically fitted to the experimental data, presented in these individually, linearized co-ordinate systems (see Eqs. (12)–(18)) and the reaction rate constant $k$ values for the all three temperatures tested were obtained. These kinetic constant $k$ values, evaluated for all assumed models, are presented in Table 3.

After some progress of the reduction reaction, the diffusion effects (resistances in mass transfer) begin to play a significant role in the overall process, influencing the sorbent's regeneration kinetics considerably. Thus, the models of the diffusion-controlled process kinetics are assumed to be valid. For the solid–gas reactions, that are diffusion controlled some kinetic models were theoretically developed based on the following assumptions: the reaction is topochemical in nature, the reaction is under diffusion control and obeys the Fick's law, one reactant diffuses into the particles of the other and the size of the particles remains unchanged during the reduction (the last one is the simplifying approach). In Table 1, four theoretically developed diffusion models ($D_1$–$D_4$, Eqs. (14)–(17)) are presented which were used for fitting the experimental data [24–26].

It was concluded above that the kinetics in the initial stage of the process for the fresh sorbent can be described using both first-order reaction model ($F_1$, Eq. (12)) and the phase-boundary controlled reaction model (for sphere, $R_3$,

Table 3
Kinetic constant $k$ calculations—kinetic region

| Lp. | Model | Cycle | $T$ (K) | $k$ ($\times 10^5$ s$^{-1}$) | Validity range ($\times 10^{-3}$ s) | Reg |
|---|---|---|---|---|---|---|
| 1 | $F_1(\alpha)$ | Fresh | 700 | 31.03 | 0–4 | 0.999 |
| 2 | $F_1(\alpha)$ | Fresh | 727 | 54.30 | 0–2 | 0.999 |
| 3 | $F_1(\alpha)$ | Fresh | 750 | 73.02 | 0–1 | 0.996 |
| 4 | $R_3(\alpha)$ | Fresh | 700 | 9.02 | 0–4 | 0.996 |
| 5 | $R_3(\alpha)$ | Fresh | 727 | 15.92 | 0–2 | 0.996 |
| 6 | $R_3(\alpha)$ | Fresh | 750 | 22.33 | 0–1 | 0.996 |
| 7 | $D_1(\alpha)$ | 5 | 700 | 8.35 | 0–5 | 0.995 |
| 8 | $D_1(\alpha)$ | 5 | 727 | 9.75 | 0–4.5 | 0.998 |
| 9 | $D_1(\alpha)$ | 5 | 750 | 24.50 | 0–2 | 0.996 |
| 10 | $D_2(\alpha)$ | 5 | 700 | 5.23 | 0–5 | 0.992 |
| 11 | $D_2(\alpha)$ | 5 | 727 | 6.14 | 0–4 | 0.994 |
| 12 | $D_2(\alpha)$ | 5 | 750 | 16.02 | 0–2 | 0.993 |
| 13 | $D_3(\alpha)$ | 5 | 700 | 1.58 | 0–7 | 0.994 |
| 14 | $D_3(\alpha)$ | 5 | 727 | 1.87 | 0–6 | 0.994 |
| 15 | $D_3(\alpha)$ | 5 | 750 | 4.60 | 0–4 | 0.993 |
| 16 | $D_4(\alpha)$ | 5 | 700 | 1.26 | 0–5 | 0.990 |
| 17 | $D_4(\alpha)$ | 5 | 727 | 1.52 | 0–5 | 0.995 |
| 18 | $D_4(\alpha)$ | 5 | 750 | 3.84 | 0–3 | 0.994 |
| 19 | $A_2(\alpha)$ | 10 | 700 | 24.65 | 0–3.8 | 0.999 |
| 20 | $A_2(\alpha)$ | 10 | 727 | 238.42 | 0–0.4 | 0.930 |
| 21 | $A_2(\alpha)$ | 10 | 750 | 463.91 | 0–0.3 | 0.972 |

Eq. (13))l. The $F_1$ model ($R = 0.999$–$0.996$) seems to provide a slightly better fit than the alternative $R_3$ model ($R = 0.996$). However based on the errors of data collection, both models could not be rejected and can be assumed to be equally valid. These models ($F_1$, $R_3$) are valid within the same time ranges, namely: $t = 0$–$4000$ s ($T = 700$ K), $t = 0$–$2000$ s ($T = 727$ K) and $t = 0$–$1000$ s ($T = 750$ K). It suggests that the active surface strongly influences the reaction course in the fresh sorbent during the initial regeneration cycles (especially concluded from the $R_3$ model). On increasing the temperature, the reaction rate is expected to increase since the enthalpy of this reaction indicates the endothermic transformation ($\Delta H^{298} = +73.4$ kJ/mol). This is visible from the kinetic constant $k$ values. On increasing $T$ from 700 to 750 K, the $k$ value increases by 2.35-times (from $k = 31.03 \times 10^{-5}$ to $73.02 \times 10^{-5}$ s$^{-1}$) for $F_1$ model and by 2.47-times (from $k = 9.02 \times 10^{-5}$ to $22.33 \times 10^{-5}$ s$^{-1}$) for $R_3$ model. As a result of the increase in the reaction rate, corresponding to the elevation of $T$ from 700 to 750 K, the kinetic region (considered as $F_1$ and $R_3$ models applicability ranges—the linear sections of Eqs. (12) and (13)—and expressed by the reaction time) shrinks considerably by 75%, from: $t = 0$–$4000$ s ($T = 700$ K) to $t = 0$–$1000$ s ($T = 750$ K). This is possibly due to the formation (relatively earlier in the elevated $T$) of the diffusion layer of the product (metallic $Cu^0$), thus, change in the step limiting mechanism.

It is observed that the ranges of applicability for the all diffusion models $D_1$–$D_4$ starts earlier with increasing temperature of the reaction, primarily due to the shrinkage of the kinetic region. However, the extent of the influence of the diffusional effects (ranges of the starting ($t = 7000$–$9000$ s) and the ending time ($t = 30{,}000$ s)) is considerably less than that observed within the kinetic region ($t = 0$–$1000$ s compared to $t = 0$–$4000$ s, for $T = 750$ and 700 K, appropriately). Considering practically the same values of the regression correlation coefficient, $R$ (e.g. $R = 0.957$–$0.965$ for $T = 700$ K, $R = 0.981$–$0.986$ for $T = 727$ K and $R = 0.963$–$0.964$ for $T = 750$ K, respectively) it seems inadequate to draw any conclusions concerning the diffusion mechanism based only on this strictly statistical information. However, one can assume some change in the diffusion mechanism with increasing $T$. For $T = 700$ K, the one-dimensional diffusion model $D_1$ fits the best to the experimental data ($R = 0.965$), while for $T = 727$ K the two-dimensional $D_2$ ($R = 0.986$) seems to be the optimal model. For the highest temperature value ($T = 750$ K), it is very difficult to distinguish between the appropriate kinetic equation since all four models $D_1$–$D_4$ are equally applicable ($R = 0.964$). According to the statistical analysis, one can only formulate the hypothesis that the diffusion mechanism changes from the one-dimensional into the three-dimensional (through the two-dimensional) with the increase in $T$ from 700 to 750 K. The difficulties concerning the discrimination in the diffusion mechanisms are presented in the Hancock and Sharp's fundamental work [24]. The comparison between the experimental data and the kinetic models predictions concerning the fresh sorbent regeneration kinetics is presented in Fig. 2.

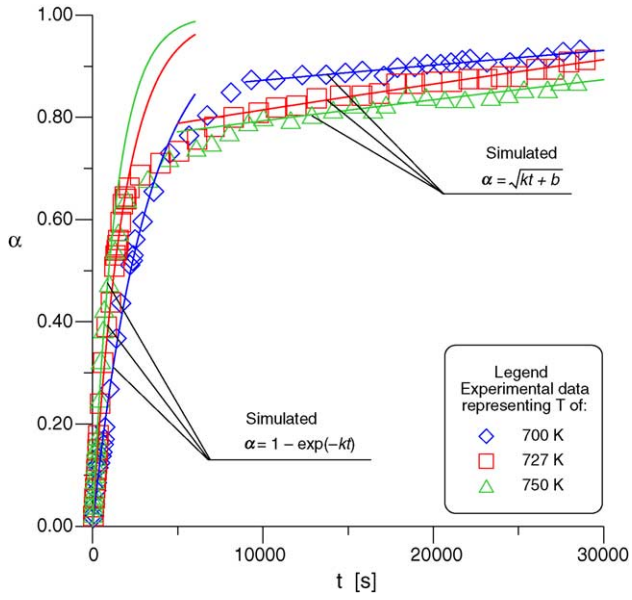


Fig. 2. Graphical comparison between experimental and modeled data, fresh sorbent, $T$ range of 700–750 K).

After the sorbent's active surface have been periodically used and renewed, the sorbent's regeneration process kinetics alters gradually. The next set of methane regeneration TGA experiments was performed using the sorbent (called intermediate) in the selected, next stage of its life (after the consecutive five sulfation and immediately followed regeneration cycles). Applying the Hancock and Sharp's procedure [24] to the recalculated experimental data (Eqs. (10) and (11)), $m = 0.4176$ was obtained. It was concluded, that this kinetics is diffusion controlled. However, the $m$ mean parameter value does not directly identify any particular diffusion model. From this reason all the models, $D_1$–$D_4$, were applied and statistically fitted to the experimental data using the regression methods (the least square method). In this case, it can be concluded that one deals with the two separate diffusion regions—the first corresponding to the initial process stage (Table 3) and the second, to the diffusion process through the surface product layer (Table 4). Considering the initial stage's data, it is seen that the process follows the one-dimensional ($D_1$) kinetics in the all three temperatures studied (for $T = 700$ K, the corresponding $R = 0.995$; for $T = 727$ K, $R = 0.998$ and for $T = 750$ K, $R = 0.996$). With an increase in temperature, the range of the initial process stage decreases, from $t = 0$–$5000$ s for $T = 700$ K to $t = 0$–$4500$ s ($T = 727$ K) and, sharply, to $t = 0$–$2000$ s for $T = 750$ K (Table 3, the one-dimensional diffusion model ($D_1$) assumed). It corresponds to the increase in the kinetic constant $k$ value ($T = 700$ K, $k = 8.346 \times 10^{-5}$ s$^{-1}$; $T = 727$ K, $k = 9.752 \times 10^{-5}$ s$^{-1}$; $T = 750$ K, $k = 24.499 \times 10^{-5}$ s$^{-1}$) (see Table 3). The next, diffusional stage follows the three-dimensional ($D_3$) diffusion mechanism as it is indicated

Table 4
Kinetic constant $k$ calculations—diffusion region

| Lp. | Model | Cycle | $T$ (K) | $k$ ($\times 10^5$ s$^{-1}$) | Validity range ($\times 10^{-3}$ s) | Reg |
|---|---|---|---|---|---|---|
| 1 | $D_1(\alpha)$ | Fresh | 700 | 0.527 | 9–30 | 0.965 |
| 2 | $D_1(\alpha)$ | Fresh | 727 | 0.849 | 8–30 | 0.984 |
| 3 | $D_1(\alpha)$ | Fresh | 750 | 0.672 | 7–30 | 0.963 |
| 4 | $D_2(\alpha)$ | Fresh | 700 | 0.678 | 9–30 | 0.963 |
| 5 | $D_2(\alpha)$ | Fresh | 727 | 0.972 | 8–30 | 0.986 |
| 6 | $D_2(\alpha)$ | Fresh | 750 | 0.713 | 7–30 | 0.964 |
| 7 | $D_3(\alpha)$ | Fresh | 700 | 0.496 | 9–30 | 0.957 |
| 8 | $D_3(\alpha)$ | Fresh | 727 | 0.595 | 8–30 | 0.981 |
| 9 | $D_3(\alpha)$ | Fresh | 750 | 0.388 | 7–30 | 0.964 |
| 10 | $D_4(\alpha)$ | Fresh | 700 | 0.228 | 9–30 | 0.961 |
| 11 | $D_4(\alpha)$ | Fresh | 727 | 0.306 | 8–30 | 0.985 |
| 12 | $D_4(\alpha)$ | Fresh | 750 | 0.216 | 7–30 | 0.964 |
| 13 | $D_1(\alpha)$ | 5 | 700 | 1.464 | 10–30 | 0.969 |
| 14 | $D_1(\alpha)$ | 5 | 727 | 1.278 | 12–30 | 0.989 |
| 15 | $D_1(\alpha)$ | 5 | 750 | 1.220 | 5–30 | 0.978 |
| 16 | $D_2(\alpha)$ | 5 | 700 | 1.646 | 10–30 | 0.975 |
| 17 | $D_2(\alpha)$ | 5 | 727 | 1.861 | 12–30 | 0.991 |
| 18 | $D_2(\alpha)$ | 5 | 750 | 1.700 | 5–30 | 0.987 |
| 19 | $D_3(\alpha)$ | 5 | 700 | 1.027 | 7–30 | 0.986 |
| 20 | $D_3(\alpha)$ | 5 | 727 | 1.670 | 6–25 | 0.996 |
| 21 | $D_3(\alpha)$ | 5 | 750 | 1.388 | 4–25 | 0.998 |
| 22 | $D_4(\alpha)$ | 5 | 700 | 0.598 | 5–25 | 0.984 |
| 23 | $D_4(\alpha)$ | 5 | 727 | 0.719 | 10–25 | 0.994 |
| 24 | $D_4(\alpha)$ | 5 | 750 | 0.623 | 3–25 | 0.994 |
| 25 | $D_1(\alpha)$ | 10 | 700 | 1.076 | 12–30 | 0.977 |
| 26 | $D_1(\alpha)$ | 10 | 727 | 0.396 | 9–30 | 0.969 |
| 27 | $D_1(\alpha)$ | 10 | 750 | 0.347 | 8–30 | 0.960 |
| 28 | $D_2(\alpha)$ | 10 | 700 | 1.417 | 12–30 | 0.982 |
| 29 | $D_2(\alpha)$ | 10 | 727 | 0.825 | 10–30 | 0.972 |
| 30 | $D_2(\alpha)$ | 10 | 750 | 0.550 | 9–30 | 0.960 |
| 31 | $D_3(\alpha)$ | 10 | 700 | 1.246 | 8–30 | 0.991 |
| 32 | $D_3(\alpha)$ | 10 | 727 | 1.767 | 6–30 | 0.977 |
| 33 | $D_3(\alpha)$ | 10 | 750 | 0.743 | 7–30 | 0.982 |
| 34 | $D_4(\alpha)$ | 10 | 700 | 0.511 | 12–30 | 0.986 |
| 35 | $D_4(\alpha)$ | 10 | 727 | 0.477 | 7–30 | 0.967 |
| 36 | $D_4(\alpha)$ | 10 | 750 | 0.247 | 6–30 | 0.980 |

statistically in Table 4 (for $T = 700$ K, the corresponding $R = 0.986$, for $T = 727$ K, $R = 0.996$ and for $T = 750$ K, $R = 0.998$). The comparison between the experimental data and the kinetic models predictions for the intermediate sorbent is presented in Fig. 3.

The regeneration kinetics of the heavily cycled sorbent (Table 3) follows the two consecutive steps. The first one, according to the Hancock and Sharp's procedure, can be described using the $A_2$ kinetic model (Avrami–Erofe'ev model of two-dimensional nucleation and crystals growth), since the Eq. (11) produces the average value of $m = 2.0706$ (see Tables 1 and 2). For the heavily cycled sorbent the regeneration process is extremely temperature-sensitive. For $T = 700$ K, the kinetic constant value is $k = 24.65 \times 10^{-5}$ s$^{-1}$, while an elevation of the temperature to $T = 727$ K leads to a considerably increase in the $k$ value ($k = 238.42 \times 10^{-5}$ s$^{-1}$, this is 9.67-times increase). Further elevation of temperature to the value of $T = 750$ K results in nearly a 19-fold increase of the kinetic constant value to $k = 463.91 \times 10^{-5}$ s$^{-1}$). In addition, with an increase in the process temperature, the kinetic region's width shrinks considerably ($t = 0$–$3800$ s cor-

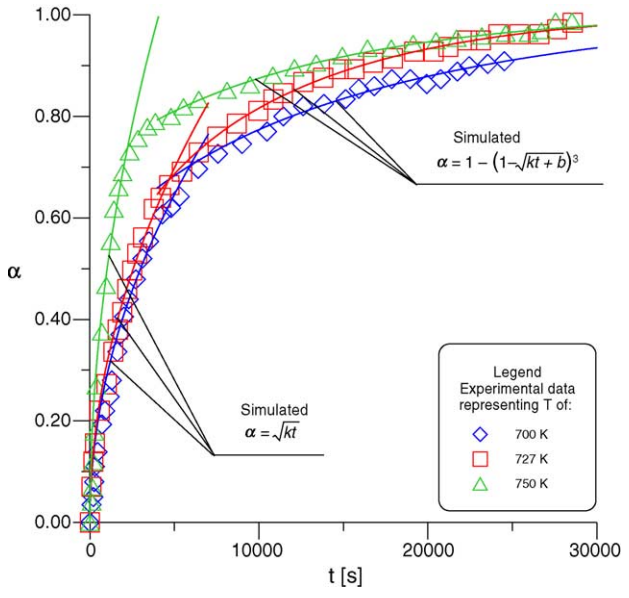


Fig. 3. Graphical comparison between experimental and modeled data, intermediate used sorbent, $T$ range of 700–750 K).

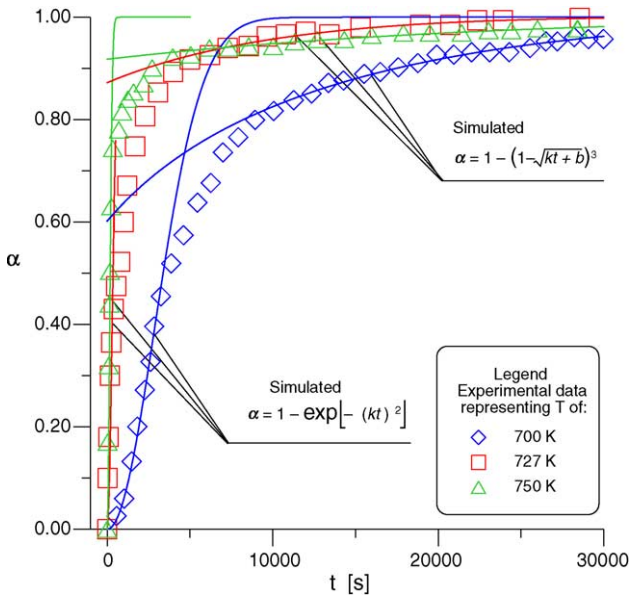


Fig. 4. Graphical comparison between experimental and modeled data, heavily used sorbent, $T$ range of 700–750 K).

responded to $T = 700$ K while the $t = 0$–300 s corresponded to $T = 750$ K). The difference between the kinetic region's width corresponding to $T = 727$ and 750 K is considerably smaller ($t = 0$–400 s and $t = 0$–300 s, respectively) in comparison to the time window corresponding to the lowest $T = 700$ K (where $t = 0$–3800 s). After the $Cu^0$ product layer is formed on the active catalytic surface, the diffusion process governs the entire process kinetics. The data from Table 4 indicate that, statistically, the three-dimensional ($D_3$) diffusion model best mimics the experimental data (as for $T = 700$ K, the correlation coefficient $R = 0.991$; for $T = 727$ K, $R = 0.977$ and for $T = 750$ K, $R = 0.982$). The comparison between the experimental data and the kinetic models predictions for the heavily cycled sorbent are presented in Fig. 4.

It is noticeable that there is a very large difference between the specific surface area of the samples at various stages of the sorbent's life (the BET 3-points measurements): fresh, 220.67 $m^2$/g; intermediate (5 cycles), 183.63 $m^2$/g and heavy used (10 cycles), 128.55 $m^2$/g. Yoo et al. [8] report the similar value of the specific surface area of the fresh sorbent (185 $m^2$/g). They reported that after bulk sulfation the pore volume of the sulfated sorbent decreased due to the pore plugging (caused by the initial formation of nonregenerable $Al_2(SO_4)_3$, residual sulfur, copper sulphate, CuO crystallites and the thermal sintering, as well) with an effective decrease of the specific surface area (to 76 $m^2$/g). When the regeneration temperature increases up to $T = 773$ K, both the pore volume and the specific surface area of the regenerated sorbent approached the value of the fresh one. Macken et al. [9] reported, however, contradictory conclusions—increase in the total pore volume and decrease in the BET specific surface area along with the number of sulfation–regeneration cycles (from 117 to 86 $m^2$/g). Deng and Lin [4] reported the decrease of the BET specific surface area from 91–123 to 62–83 $m^2$/g after 5 cycles. The reported data were interpreted by the sintering phenomena and simple kinetic model of the specific surface area reduction was reported with the activation energy of sintering introduced and estimated in the range of 101.5–121.3 kJ/mol. Some similar variations in the surface area of vanadia-alumina catalysts exposed to $SO_2$ were reported by Nam et al. [27]. They explained this phenomenon to be the result of the volume expansion in the $\gamma$-$Al_2O_3$ as the sulfation proceeds which causes plugging of the pores of $\gamma$-$Al_2O_3$ support, Yoo et al. [28] observed that the decrease in surface area of 2 wt.% CuO impregnated $\gamma$-$Al_2O_3$sorbent exposed to 1 vol.% $SO_2$ at $T = 773$ K was about 20% after 1 h, whereas the surface area of 8 wt.% CuO impregnated $\gamma$-$Al_2O_3$ sorbent decreased over the course of 7 h by about 65%. The presented data can be explained by the fact, that there is a molecular volume expansion while copper sulfate is formed from copper oxide, which causes pore plugging and thus resukts in a decrease in the active surface (from 220.67 to 183.63 $m^2$/g (by 16.78%) for intermediate age and to 128.55 $m^2$/g (by 41.74%) for the strongly aged one). It also indirectly affects the adsorption capabilities of the sorbent. Due to these complex phenomena interactions, as the life of the sorbent goes up, the regeneration kinetics slowly shifts from the $F_1/R_3$ mechanisms (fresh sorbent) towards the diffusion-controlled mechanisms ($D_1$–$D_4$) (intermediate sorbent). As the regeneration efficiency goes slowly down, the $CuSO_4$ present in the surface layer forms a major part of the regenerated sorbent. The creation of CuO crystallites, reported by some researchers, becomes the main kinetic mechanism in the heavy cycled sorbent, which can be modeled by the Avrami–Erofe'ev two-dimensional nucleation and crystal growth model $A_2$.

The kinetic constant $k$ values corresponding to the second (diffusion) stage of the each examined regeneration process (independently on the sorbent life cycle) incorporate in their "effective" values the three main diffusion mechanisms: diffusion through the product layer formed (resulting from the process course), internal diffusion through the $\gamma$-$Al_2O_3$ support pores and the counterdiffusion of volatile reaction products ($SO_2$, $CO_2$ and $H_2O$)l.

The agreement between the $n$ values of conversion degree ($\alpha^{calc}$)—calculated using the selected kinetic models assumed and the $n$ values of the experimental data ($\alpha^{exp}$) was determined statistically by calculating the mean deviation (MD):

$$MD = \frac{\sum(\alpha^{calc} - \alpha^{exp})}{n} \quad (19)$$

as well as the root mean square deviation (RMSD):

$$RMSD = \sqrt{\frac{\sum(\alpha^{calc} - \alpha^{exp})^2}{n-1}} \quad (20)$$

The statistical calculations results are summarized in Table 5.

Table 5
Statistical quality of the developed kinetic models—MD and RMSD values

| Lp. | Model | Cycle | $T$ (K) | Region | MD | RMSD |
|---|---|---|---|---|---|---|
| 1 | $F_1(\alpha)$ | Fresh | 700 | Kinetic | −0.00229 | 0.01589 |
| 2 | $F_1(\alpha)$ | Fresh | 727 | Kinetic | −0.00231 | 0.01401 |
| 3 | $F_1(\alpha)$ | Fresh | 750 | Kinetic | $-7.98 \times 10^{-5}$ | 0.01465 |
| 4 | $R_3(\alpha)$ | Fresh | 700 | Kinetic | −0.01139 | 0.02206 |
| 5 | $R_3(\alpha)$ | Fresh | 727 | Kinetic | −0.00595 | 0.02386 |
| 6 | $R_3(\alpha)$ | Fresh | 750 | Kinetic | −0.00470 | 0.01694 |
| 7 | $D_1(\alpha)$ | Fresh | 700 | Diffusion | 0.01246 | 0.03564 |
| 8 | $D_1(\alpha)$ | Fresh | 727 | Diffusion | 0.01089 | 0.02772 |
| 9 | $D_1(\alpha)$ | Fresh | 750 | Diffusion | 0.02754 | 0.06512 |
| 10 | $D_1(\alpha)$ | 5 | 700 | Kinetic | 0.02886 | 0.04271 |
| 11 | $D_1(\alpha)$ | 5 | 727 | Kinetic | 0.01042 | 0.01834 |
| 12 | $D_1(\alpha)$ | 5 | 750 | Kinetic | 0.03880 | 0.06680 |
| 13 | $D_3(\alpha)$ | 5 | 700 | Diffusion | 0.00377 | 0.01439 |
| 14 | $D_3(\alpha)$ | 5 | 727 | Diffusion | 0.00039 | 0.00524 |
| 15 | $D_3(\alpha)$ | 5 | 750 | Diffusion | 0.00174 | 0.00870 |
| 16 | $A_2(\alpha)$ | 10 | 700 | Kinetic | 0.00741 | 0.02999 |
| 17 | $A_2(\alpha)$ | 10 | 727 | Kinetic | −0.05017 | 0.13258 |
| 18 | $A_2(\alpha)$ | 10 | 750 | Kinetic | −0.01263 | 0.12117 |
| 19 | $D_3(\alpha)$ | 10 | 700 | Diffusion | 0.01731 | 0.04473 |
| 20 | $D_3(\alpha)$ | 10 | 727 | Diffusion | 0.07244 | 0.14726 |
| 21 | $D_3(\alpha)$ | 10 | 750 | Diffusion | 0.02085 | 0.04506 |

The kinetic data were also further elaborated to estimate the activation energy values. The ln ($k$) versus $1/T$ is a straight line relationship with negative slope (Arrhenius equation) [29]:

$$k = c \exp\left(-\frac{\Delta E_a}{RT}\right) = c \exp\left(-\frac{\Delta E_a}{8.314T}\right) \quad (21)$$

$$\ln k = -\frac{\Delta E_a}{R} \times \frac{1}{T} + \ln c \quad (22)$$

The recalculated data are presented in the Table 6. These indicate that the activation energy increases with an increase in the age of the sorbent (slightly between the fresh ($\Delta E_a$ = 75–80 kJ/mol) and the intermediate one-after 5 cycles ($\Delta E_a$ = 90 kJ/mol), while considerably between the intermediate (5 cycled) and the heavy used one (10 cycled) ($\Delta E_a$ = 260 kJ/mol)). The heavily used sorbent, with the highest activation energy value, is very temperature sensitive as it was indicated in the previous paragraph (see also Fig. 4). Macken and Hodnett [9] reported a lower value of activation energy ($\Delta E_a$ = 60.4 kJ/mol) for the reduction of the sulfated CuO on γ-$Al_2O_3$ support sample with $H_2$. Kiel et al. [30] found that the activation energy value for the reduction of pure $CuSO_4$ with $H_2$ was between 62 and 70 kJ/mol, while for the reduction of sulfated CuO on $SiO_2$ support it was $\Delta E_a$ = 72 kJ/mol. The apparent activation energy value for the reduction of sulfated CuO on γ-$Al_2O_3$ with $CH_4$ was found to be $\Delta E_a$ = 116 kJ/mol. For the same regeneration reaction Yeh et al. [17] obtained the value of 108.6 kJ/mol. It compares favorably with the authors own data set, as these values are mostly within the activation energy window obtained in the presented study. Besides, it should be emphasized that although the various kinetic models were used for the each stage of the sorbent's life independently, the activation energy values obtained for each sorbent are practically equal (e.g. the fresh sorbent: $\Delta E_a$ = 75–79 kJ/mol, intermediate sorbent: $\Delta E_a$ = 90–94 kJ/mol). Harriott and Markussen [7] reported the (apparent) activation energy value of 100 kJ/mol between $T$ = 723 and 753 K and $\Delta E_a$ = 75 kJ/mol between $T$ = 753 and 783 K. The decrease in the activation energy value was explained by them in the terms of the thermal effects in the pore diffusion processes.

Table 6
Activation energy calculations

| Lp. | Model | $c$ ($s^{-1}$) | $\Delta E_a$ (kJ/mol) | Reg |
|---|---|---|---|---|
| 1 | $F_1(\alpha)$ | 131.15 | 75.250 | 0.993 |
| 2 | $R_3(\alpha)$ | 78.84 | 79.510 | 0.997 |
| 3 | $D_1(\alpha)$ | 457.46 | 91.065 | 0.898 |
| 4 | $D_2(\alpha)$ | 532 | 94.700 | 0.898 |
| 5 | $D_3(\alpha)$ | 76.8 | 90.330 | 0.904 |
| 6 | $D_4(\alpha)$ | 119.47 | 94.230 | 0.908 |
| 7 | $A_2(\alpha)$ | $8.034 \times 10^{15}$ | 260.400 | 0.971 |

## 4. Conclusions

The used sorbent regeneration is an important step in the copper oxide flue gas cleanup processes. Poor regeneration performance could require higher sorbent circulation rate, resulting in the considerably increase in the process costs. It was found, that the regeneration kinetics of CuO on γ-$Al_2O_3$ sorbent follows the apparently first-order and phase-boundary controlled reaction kinetics when the life of the sorbent is short (e.g. the fresh sample). When the sorbent's age increases, the reaction mechanism shifts to the diffusion control first (intermediate sorbent), and then to two-dimensional nucleation and crystal growth (of CuO crystallites). The autocatalytic behavior of this reaction produces the resulting

sigmoidal shape of the $\alpha = f(t)$ curve due to the diffusional effects on the overall kinetics. This confirms the findings reported by Macken et al. [1]. Thus, this course is very similar to the one resulted from the topochemical phase transformations (Avrami–Erofe'ev model of nucleation and crystal growth of the large CuO crystallites).

In each of sorbents age analyzed, the reaction rate increases with the increasing $T$—there is no visible or confirmable change in the reaction mechanism within the $T = 700$–$750$ K range.

Based on the BET measurements of the specific surface area, it was found that the available (thus active) specific surface area decreases with the sorbent's age. This can be attributed, among some other factors, to the volume expansion of the surface copper sulfate and generation of the large CuO crystallites. This causes pore plugging and copper sulfate trapping inside the pores. However, there are some reports about the advantages of these complex phenomena such as the improvement of the dispersion (redispersion) of the supported active CuO phase. This re-dispersion can compensate the plugging and trapping effect [1]. This fact can explain the conclusion that in the presented study there was no evidence of the sudden deactivation of catalytic properties of the sorbent.

## References


[1] C. Macken, B.K. Hodnett, G. Paparatto, Ind. Eng. Chem. Res. 39 (2000) 3868–3874.
[2] S.M. Jeong, S.D. Kim, Ind. Eng. Chem. Res. 36 (1997) 5425–5431.
[3] Z.M. Wang, Y.S. Lin, Ind. Eng. Chem. Res. 37 (12) (1998) 4675–4681.
[4] S.G. Deng, Y.S. Lin, Ind. Eng. Chem. Res. 35 (1996) 1429–1437.
[5] G. Centi, A. Riva, N. Passarini, G. Brambilla, B.K. Hodnett, B. Delmon, M. Ruwet, Chem. Eng. Sci. 45 (8) (1990) 2679–2686.
[6] G. Centi, N. Passarini, S. Perathoner, A. Riva, Ind. Eng. Chem. Res. 31 (1992) 1956–1963.
[7] P. Harriott, J.M. Markussen, Ind. Eng. Chem. Res. 31 (1992) 373–379.
[8] K.S. Yoo, S.M. Jeong, S.D. Kim, S.B. Park, Ind. Eng. Chem. Res. 35 (1996) 1543–1549.
[9] C. Macken, B.K. Hodnett, Ind. Eng. Chem. Res. 37 (1998) 2611–2617.
[10] G. Centi, N. Passarini, S. Perathoner, A. Riva, in: L. Guczi (Ed.), Combined $DeSO_x/DeNO_x$ Reactions on a Copper on Alumina Sorbent-Catalyst, Elsevier Science Publication, Amsterdam, 1993, p. 2677.
[11] H. Karge, L. Dalla, J. Phys. Chem. 88 (1984) 1538.
[12] G. Centi, B.K. Hodnett, P. Jaeger, C. Macken, M. Marella, M. Tomaselli, G. Paparatto, S. Perathoner, J. Mater. Res. 10 (1995) 553.
[13] D.H. McCrea, A.J. Forney, J.G. Myers, Recovery of sulfur from flue gases using a copper oxide adsorbent, J. Air Pollut. Control Assoc. 20 (12) (1970) 819.
[14] J.T. Yeh, J.Pl. Strakey, J.I. Joubert, $SO_2$ Absorption and Regeneration Kinetics Employing Supported Copper Oxide. Pittsburgh Energy Technology Center, Pittsburgh, PA, 1987, Unpublished paper.
[15] D.H. McCrea, J.G. Myers, A.J. Forney, Evaluation of solid absorbents for sulfur oxides removal from stack gases, in: Proceedings of Second International Clean Air Congress, Academic, New York, 1971, p. 922.
[16] J.T. Yeh, R.J. Demski, J.P. Strakey, J.I. Joubert, Combined $SO_2/NO_x$ removal from flue gas, Environ. Prog. 4 (4) (1985) 223–228.
[17] G. Centi, N. Passarini, S. Perathoner, A. Riva, Ind. Eng. Chem. Res. 31 (1992) 1947–1955.
[18] H. Johannes, A.V. Heldon, J.E. Naber, Inter. Patent Specification B 01 j 11/32; C 01 b 17/60, 1969.
[19] J.H.A. Kiel, W. Prins, W.P.M. van Swaaij, Appl. Catal. B: Environ. 1 (1) (1992) 13–39.
[20] S.M. Jeong, S.D. Kim, Ind. Eng. Chem. Res. 36 (12) (1997) 5425–5431.
[21] J.T. Yeh, C.J. Drummond, J.I. Joubert, Environ. Prog. 6 (1987) 44–50.
[22] Z.Y. Chen, J.T. Yeh, Environ. Prog. 17 (2) (1998) 61–69.
[23] R. Vishnuraj, A Kinetic Study for the Regeneration of Copper Oxide Sorbent by Methane. Master Thesis, Dep. of Mech. Eng. and Energy Proc., Southern Illinois University at Carbondale, Carbondale, IL, USA, 1999.
[24] J.D. Hancock, J.H. Sharp, Method of comparing solid-state kinetic data and its application to the Cecomposition of Kaolinite, Brucite, and $BaCO_3$, J. Amer. Ceram. Soc. 55 (1972) 74.
[25] R.A. Gardner, The kinetics of silica reduction in hydrogen, J. Solid State Chem. 9 (1974) 336–344.
[26] H. Wang, W.J. Thomson, AIChE J. 41 (7) (1995) 1790–1797.
[27] I.S. Nam, J.W. Eldridge, J.R. Kittrell, Deactivation of Vanadia-Alumina catalyst for NO reduction by $NH_3$, Ind. Eng. Chem. Prod. Res. Dev. 25 (1986) 192.
[28] K.S. Yoo, S.D. Kim, S.B. Park, Sulfation of $Al_2O_3$ in flue gas desulfurization by CuO/γ-alumina sorbent, Ind. Eng. Chem. Res. 33 (1994) 1786.
[29] O. Levenspiel, Chemical Reactor Engineering, second ed., John Wiley & Sons, New York, 1972.
[30] J.H.A. Kiel, W. Prins, W.P.M. van Swaaij, Performance of silica-supported copper oxide sorbents for $SO_2/NO_x$ removal from flue gas. Part I, Appl. Catal. B 1 (1992) 13.